COMPONENT PART NOTICE

THIS PAPER IS A COMPONENT PART OF THE FOLLOWING COMPILATION REPORT:

(TITLE): The Effect of the Ionosphere on Radiowave Signals and Systems Performance Based on Ionospheric Effects Symposium Held on 1-3 May 1990.

(SOURCE): Naval Research Lab., Washington, DC

TO ORDER THE COMPLETE COMPILATION REPORT USE AD-A233 797.

THE COMPONENT PART IS PROVIDED HERE TO ALLOW USERS ACCESS TO INDIVIDUALLY AUTHORED SECTIONS OF PROCEEDINGS, ANNALS, SYMPOSIA, ETC. HOWEVER, THE COMPONENT SHOULD BE CONSIDERED WITHIN THE CONTEXT OF THE OVERALL COMPILATION REPORT AND NOT AS A STAND-ALONE TECHNICAL REPORT.

THE FOLLOWING COMPONENT PART NUMBERS COMPRISE THE COMPILATION REPORT:

AD#:	TITLE:
AD-P006 265 thru AD-P006 325	

Accesion For	
NTIS CRA&I	☑
DTIC TAB	☐
Unannounced	☐
Justification	
By	
Distribution/	
Availability Codes	
Dist	Avail and/or Special
A-1	

A GENERAL CHANNEL MODEL FOR RF PROPAGATION THROUGH STRUCTURED IONIZATION

Roger A. Dana
Mission Research Corporation
Santa Barbara, California

Leon A. Wittwer
Defense Nuclear Agency
Washington, D.C.

INTRODUCTION

Design and evaluation of radio frequency (RF) systems that must operate through ionospheric disturbances resulting from high altitude nuclear detonations requires an accurate channel model. Such a model can be used to construct realizations of the received signal for use in digital simulations of transionospheric communications links and radars or for use in hardware channel simulators.

It is well known that the first order statistics of the received RF signal after propagation through strongly scattering ionospheric disturbances are accurately described by the Rayleigh probability distribution for the amplitude and a uniform distribution for the phase. Equivalently, the two orthogonal components of the received electric field are independent, zero mean normal random processes. Given the second order statistics of the received signal, standard statistical techniques can be used to generate realizations of the channel impulse response function from which the received signal can be constructed.

The second order statistics of transionospheric RF scintillation are described by the two-position, two-frequency, two-time mutual coherence function of the received signal. The derivation of the mutual coherence function, which is a solution of Maxwell's equations, requires a model for the temporal and spatial variations of the electron density fluctuations in the ionosphere. Under Taylor's frozen-in hypothesis, the electron density fluctuations are described as a rigid structure that drifts past the line-of-sight. There is then a deterministic relationship between spatial and temporal fluctuations in the electron density. This model is accurate when the ionization has formed a thin layer of striations aligned with the geomagnetic field lines. Before striations have formed or when there are multiple scattering layers in the ionosphere with different relative velocities, a turbulent model may be more appropriate. In the fully turbulent case, the spatial and temporal fluctuations of the electron density are uncorrelated. Reality should lie somewhere between these two limiting models.

This paper describes a general model which varies smoothly between the frozen-in and turbulent models. The starting point for the general model is a description of the electron density fluctuations in the ionosphere that includes space-time correlation. Then the mutual coherence function for the general model is presented. Examples are given which illustrate the effects on the received signal due to the variation from the turbulent to frozen-in models.

MUTUAL COHERENCE FUNCTION

The derivation of the mutual coherence function starts with Maxwell's equations from which the parabolic wave equation is derived. The parabolic wave equation can be solved to give the received electric field for a specific electron density distribution in the ionosphere. However, the electron density distribution is a random process so the received electric field is also a random process. The parabolic wave equation is therefore used to derive an equation for the two-position, two-frequency, two-time mutual coherence function of the electric field, $\Gamma(\Delta\mathbf{r},\Delta\omega,\Delta t)$. The solution of the differential equation for Γ, which is also a solution of Maxwell's equations, then provides a description of the second-order statistics of the received electric field. The Fourier transform of the mutual coherence function is the Generalized Power Spectral Density (GPSD) of the received signal.

Consider a monochromatic spherical wave with an electric field $E(\mathbf{r},\omega,t)$ which is a function of position $\mathbf{r}$, carrier radian frequency ω, and time t. The wave originates from a transmitter located at $\mathbf{r} = (0,0,-z_t)$ and propagates in free space in the positive z direction until it is incident on an irregularly ionized layer which extends from $0 < z < L$ and is infinite in the x-y plane. After emerging from the layer at $z = L$, the wave propagates in free space to a receiver located at $\mathbf{r} = (0,0,z_r)$. This geometry is illustrated in Figure 1. As the wave propagates, its phase varies as $i\omega t - i\langle k\rangle z$, so we can write

$$E(\mathbf{r},\omega,t) = U(\mathbf{r},\omega,t)\exp\left[i\left(\omega t - \int_{-z_t}^{z}\langle k(z')\rangle\, dz'\right)\right] \tag{1}$$

where

$$\langle k\rangle^2 = \frac{\omega^2}{c^2}\left[1 - \frac{4\pi r_e c^2\langle n_e\rangle}{\omega^2}\right], \tag{2}$$

c is the speed of light in a vacuum, $\langle n_e\rangle$ is the mean free electron density in the ionosphere, and r_e is the classical electron radius. Under the small angle scattering assumption, it can be shown that U obeys the parabolic wave equation [Tatarskii 1971]:

$$\nabla_\perp^2 U - 2i\langle k\rangle\frac{\partial U}{\partial z} - \langle k\rangle^2\left[1 - \frac{4\pi r_e c^2 n_e(\mathbf{r},t)}{\omega^2}\right]U = 0 \tag{3}$$

where $n_e(\mathbf{r},t)$ is the free electron density which is a function of space and time.

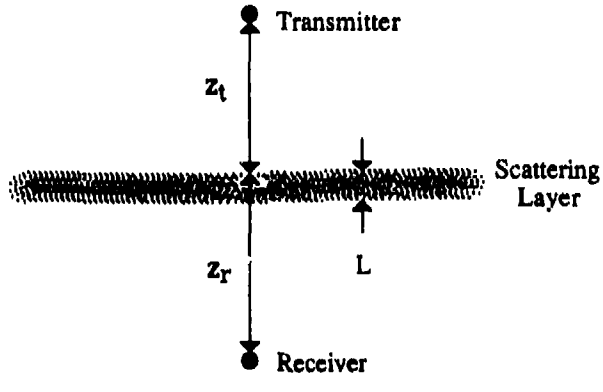

Figure 1. Propagation geometry.

The statistical nature of $n_e(r,t)$ requires a statistical approach to solving the parabolic wave equation. Thus a differential equation for the mutual coherence function,

$$\Gamma(\Delta r,\Delta\omega,\Delta t) = \langle U(r_1,\omega_1,t_1)U^*(r_2,\omega_2,t_2)\rangle \tag{4}$$

is derived from the parabolic wave equation assuming small angle scattering, wide-sense statistically stationary processes, and a model for the temporal fluctuations of n_e. The details of this derivation may be found in Tatarskii [1971] or Dana [1986].

The solution of the differential equation for the mutual coherence function depends on structure function $A(\rho)$ [Sreenivasiah, Ishimaru, and Hong 1976]:

$$A(\rho) = \int_{-\infty}^{\infty} \exp(i\mathbf{K}_\perp\cdot\rho)\, S_e(\mathbf{K}_\perp,K_z=0)\, \frac{d^2\mathbf{K}_\perp}{(2\pi)^2} \tag{5}$$

where ρ is a position vector in a plane normal to the line-of-sight with components x and y, and $S_e(\mathbf{K})$ is the three-dimensional power spectral density of the electron density fluctuations in the ionosphere. The structure function is then the correlation of the electron density fluctuations in a plane normal to the propagation direction. It is these fluctuations that cause diffraction and scintillation in the received signal. A power-law form for S_e is usually assumed [Wittwer 1979] which results in a Bessel function form for the structure function. Because the structure function occurs in the exponent of the solution for the mutual coherence function, the quadratic phase approximation is made to produce a mathematically tractable result. This quadratic phase approximation simplifies the expression for $A(\rho)$ to

$$A(\rho) = A_0\left[1 - A_2\left(\frac{x^2}{L_x^2} + \frac{y^2}{L_y^2}\right)\right]. \tag{6}$$

The constants A_0 and A_2 are determined by functional form of S_e and by the phase variance imparted on the wave in the ionosphere. The quantities L_x and L_y are electron density fluctuation scale sizes in the plane normal to the line-of-sight.

Although much information is available on the spatial fluctuations of n_e (see, for example, Wittwer 1979), there is little information on small time-scale fluctuations of n_e. Thus S_e does not, in general, contain Doppler frequency information, and a model is required to describe the temporal fluctuations. A general model for temporal dependence of the quadratic form of the structure function is

$$A(\rho,t) = A_0\left[1 - A_2\left(\frac{x^2}{L_x^2} + \frac{y^2}{L_y^2} + \frac{t^2}{T_0^2} - 2\frac{C_{xt}\,xt}{L_xT_0} - 2\frac{C_{yt}\,yt}{L_yT_0}\right)\right]. \tag{7}$$

The quantity T_0 can be thought of as a "decorrelation time" of the electron density fluctuations in the ionosphere. The degree of space-time correlation is determined by the coefficients C_{xt} and C_{yt}.

This form for the structure function reduces to the frozen-in model if, for example, C_{xt} is set to unity and C_{yt} is set to zero. Then the x dependence can be written as $(x-vt)^2/L_x^2$ where the velocity is equal to L_x/T_0. The turbulent model corresponds to the case where both C_{xt} and C_{yt} are zero.

Given a quadratic form for the structure function, a closed-form solution can be obtained for the mutual coherence function [Knepp 1983, Dana 1986]. This solution reduces to a mathematically tractable form when it is assumed that the scattering occurs in a thin layer. With these assumptions, the mutual coherence function for the general model is

$$\Gamma(x,y,\omega,t) = \frac{\exp\left[-\frac{1}{2}\left(\frac{\sigma_\phi \omega}{\omega_0}\right)^2\right] \exp\left[-(1 - C_{xt}^2 - C_{yt}^2)\left(\frac{t}{\tau_0}\right)^2\right]}{\left[1 + i\,\frac{\omega \Lambda_x}{\omega_{coh}}\right]^{\frac{1}{2}} \left[1 + i\,\frac{\omega \Lambda_y}{\omega_{coh}}\right]^{\frac{1}{2}}}$$

$$\times \exp\left[-\frac{\left(\frac{x}{\ell_x} - C_{xt}\frac{t}{\tau_0}\right)^2}{1 + i\,\frac{\omega \Lambda_y}{\omega_{coh}}}\right] \exp\left[-\frac{\left(\frac{y}{\ell_y} - C_{yt}\frac{t}{\tau_0}\right)^2}{1 + i\,\frac{\omega \Lambda_x}{\omega_{coh}}}\right] \tag{8}$$

where σ_ϕ is the standard deviation of the phase fluctuations imparted on the wave in the ionosphere, ω_0 is the angular frequency of the RF carrier, and

$$\Lambda_x = \left[\frac{2\ell_x^4}{\ell_x^4 + \ell_y^4}\right]^{\frac{1}{2}} \qquad \Lambda_y = \left[\frac{2\ell_y^4}{\ell_x^4 + \ell_y^4}\right]^{\frac{1}{2}} . \tag{9}$$

The decorrelation distances ℓ_x and ℓ_y are given by the expressions

$$\ell_x = \frac{(z_t + z_r)L_x}{z_t \sigma_\phi \sqrt{A_2}} \qquad \ell_y = \frac{(z_t + z_r)L_y}{z_t \sigma_\phi \sqrt{A_2}} , \tag{10}$$

the decorrelation time is given by the expression

$$\tau_0 = \frac{T_0}{\sigma_\phi \sqrt{A_2}} , \tag{11}$$

and the coherence bandwidth ω_{coh} is given by the expression

$$\omega_{coh} = \frac{\Lambda_y \omega_0^2 L_x^2}{2c\sigma_\phi^2 A_2} \frac{z_t + z_r}{z_t z_r} . \tag{12}$$

GENERALIZED POWER SPECTRAL DENSITY

The generalized power spectral density $S(K_\perp,\tau,\omega_D)$ of the signal incident on the plane of the receiver is the Fourier transform of the mutual coherence function:

$$S(K_\perp,\tau,\omega_D) = \int_{-\infty}^{\infty} d^2\rho \int_{-\infty}^{\infty} \frac{d\omega}{2\pi} \int_{-\infty}^{\infty} dt\, \Gamma(\rho,\omega,t) \exp\left[-i(K_\perp \cdot \rho - \omega\tau - \omega_D t)\right] \tag{13}$$

where angle-of-arrival $K_\perp$ is the Fourier transform pair of position ρ in the x-y plane, delay τ is the Fourier transform pair of relative carrier frequency ω, and Doppler frequency ω_D is the Fourier transform pair of relative time t. The quantity $S(K_\perp,\tau,\omega_D)(d^2K_\perp/4\pi^2)d\tau(d\omega_D/2\pi)$ is equal to the mean signal power arriving with angles-of-arrival in the interval $K_\perp/4\pi^2$ to $(K_\perp+d^2K_\perp)/4\pi^2$, with delays relative to a nominal propagation time in the interval τ to $\tau+d\tau$, and with Doppler frequencies in the interval $\omega_D/2\pi$ to $(\omega_D+ d\omega_D)/2\pi$. The delay dependence of the GPSD is a consequence of the fact that some of the signal energy takes a dog-leg path through the ionosphere from the transmitter to the receiver and arrives later than the signal energy that propagates straight through the ionosphere.

In general, the GPSD can be written as the product of a Doppler spectrum $S_D(\omega_D)$ and an angle-delay spectrum $S_{K\tau}(K_\perp,\tau)$:

$$S(K_\perp,\tau,\omega_D) = S_D(\omega_D)\ S_{K\tau}(K_\perp,\tau)\ . \tag{14}$$

After performing the integrals indicated in Equation 13, the Doppler spectrum for the general model is

$$S_D(\omega_D) = \frac{\sqrt{\pi}\tau_0}{\sqrt{1 - C_{xt}^2 - C_{yt}^2}} \exp\left[-\frac{(\tau_0\omega_D - C_{xt}K_x\ell_x - C_{yt}K_y\ell_y)^2}{4(1 - C_{xt}^2 - C_{yt}^2)}\right] \tag{15}$$

In terms of the components of $K_\perp$ (K_x and K_y), the angle-delay part of the GPSD is

$$S_{K\tau}(K_x,K_y,\tau) = \left[\frac{\pi}{2}\right]^{\frac{1}{2}} \ell_x\ell_y\,\alpha\omega_{coh} \exp\left[-\frac{K_x^2\ell_x^2}{4} - \frac{K_y^2\ell_y^2}{4}\right]$$

$$\times \exp\left\{-\frac{\alpha^2}{2}\left[\omega_{coh}\tau - \frac{\Lambda_y(K_x^2+K_y^2)\ell_x^2}{4}\right]^2\right\} \tag{16}$$

where the delay parameter α is defined to be

$$\alpha = \frac{\omega_0}{\sigma_\phi\omega_{coh}}\ . \tag{17}$$

The value of α is quite large under strong scattering conditions. The components of $K_\perp$ are related to the scattering angles θ_x and θ_y about the x and y axis respectively by the relations

$$K_x = \frac{2\pi\sin(\theta_x)}{\lambda} \qquad K_y = \frac{2\pi\sin(\theta_y)}{\lambda}\ . \tag{18}$$

It should be noted that the range of delay in Equation 16 is from $-\infty$ to $+\infty$. However, this delay is relative to some nominal propagation time, and the value of the GPSD rapidly approaches zero for decreasing negative values of $\omega_{coh}\tau$. In the limit that α is infinity, the GPSD is non-zero only for positive values of delay. Thus Equation 16 presents no real problem with causality.

It is interesting to examine the limits of the general model Doppler spectrum in order to show that this model does indeed encompass both the frozen-in and fully turbulent models. These limits for the Doppler spectra are:

$$\underset{\substack{C_{xt}\to 1\\ C_{yt}\to 0}}{\text{Limit}}\ S_D(\omega_D) = 2\pi\,\tau_0\,\delta(\tau_0\omega_D - K_x\ell_x) \qquad \text{(Frozen-in Model)} \tag{19}$$

and

$$\underset{\substack{C_{xt}\to 0\\ C_{yt}\to 0}}{\text{Limit}}\ S_D(\omega_D) = \sqrt{\pi}\,\tau_0 \exp\left[-\frac{\tau_0^2\omega_D^2}{4}\right]\ . \qquad \text{(Turbulent Model)} \tag{20}$$

For the frozen-in model, the delta-function relationship between Doppler frequency and K_x is what is obtained by assuming that the random diffraction pattern of the signal is "frozen" and drifts in the x direction past the receiver. For the turbulent model, the Doppler spectrum is independent of $K_\perp$ so the temporal and spatial variations in the received signal are also independent.

When the two decorrelation distances are equal ($\ell_x = \ell_y = \ell_0$), the scattering is isotropic about the line-of-sight, and the GPSD takes a somewhat simpler form. A three-dimensional plot of the isotropic one-dimension angle-delay part of the GPSD (Equation 16 integrated over one component of $K_\perp$) is shown in Figure 2. This plot shows the mean received power density as a function of normalized angle $K\ell_0$ and normalized delay $\omega_{coh}\tau$. The vertical axis is linear with arbitrary units.

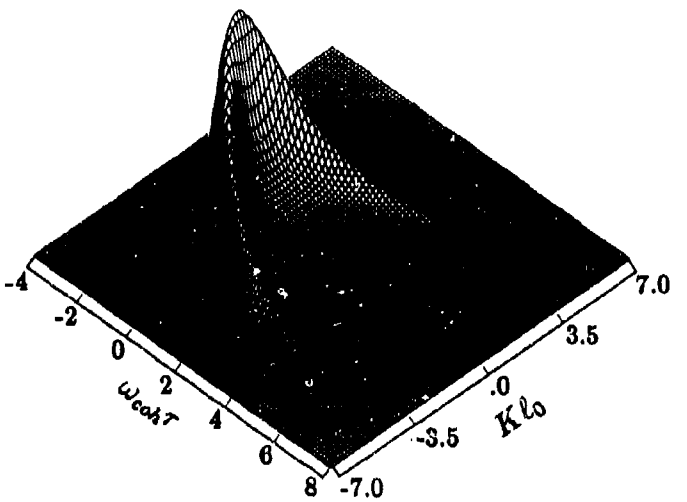

Figure 2. Angle-delay generalized power spectral density.

It can be seen that the power arriving at large angles is also the power arriving at long delays. The power arriving at long delays thus has higher spatial frequency components than power arriving at short delays. When there is strong space-time correlation (i.e. when $\sqrt{C_{xt}^2 + C_{yt}^2}$ is approximately equal to unity) these higher spatial frequency components correspond to higher Doppler frequency components. The signal arriving at long delays then varies more rapidly in time than the signal arriving at short delays.

Another view of the GPSD can be obtained by considering the delay-Doppler scattering function (Equation 14 integrated over $K_\perp$). For the turbulent model, the scattering function is separable into a function of Doppler frequency times a function of delay. This is not the case for the frozen-in model.

A comparison of the scattering functions for the frozen-in and turbulent models is shown in Figure 3. The frozen-in scattering function is just a reproduction of Figure 2 with normalized angle $K\ell_0$ replaced with normalized Doppler frequency $\tau_0\omega_D$. This is a consequence of the delta-function relationship between angle and Doppler frequency for the frozen-in model. For this model the signal at long delays has correspondingly large Doppler shifts, and a wing-like structure is seen in the scattering function. The turbulent model scattering function does not exhibit these Doppler wings because the Doppler spectrum is the same at all delays. Both functions have exactly the same power density at each delay. The difference in appearance of the figures is due to the fact that the turbulent model signal at long delay is more spread out in Doppler frequency and is therefore less obvious.

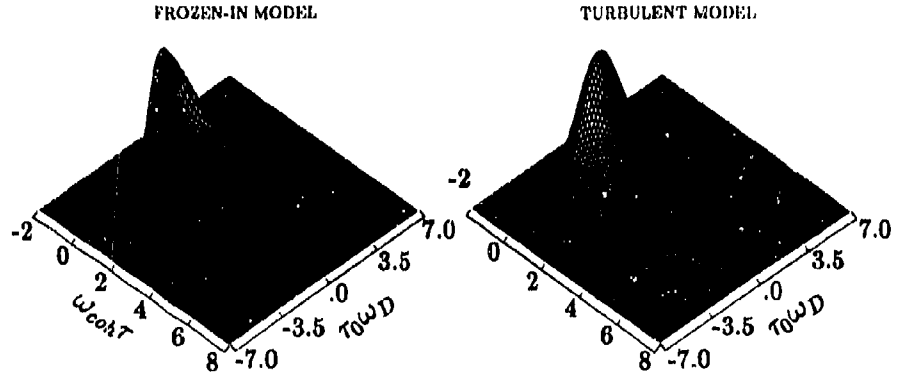

Figure 3. Comparison of scattering functions for the frozen-in and turbulent models.

A progression of scattering functions for the general model is shown in Figure 4. The space-time correlation coefficient C_{xt} varies from 0.99 for the scattering function in the upper left to 0.7 for the scattering function in the lower right. The scattering function for C_{xt} equal to 0.99 is essentially identical to that for the frozen-in model, and the scattering function for C_{xt} equal to 0.7 is essentially identical to that for the turbulent model. For intermediate values of C_{xt}, the scattering functions still exhibit Doppler wings but the wings have broader Doppler spectra as C_{xt} decreases.

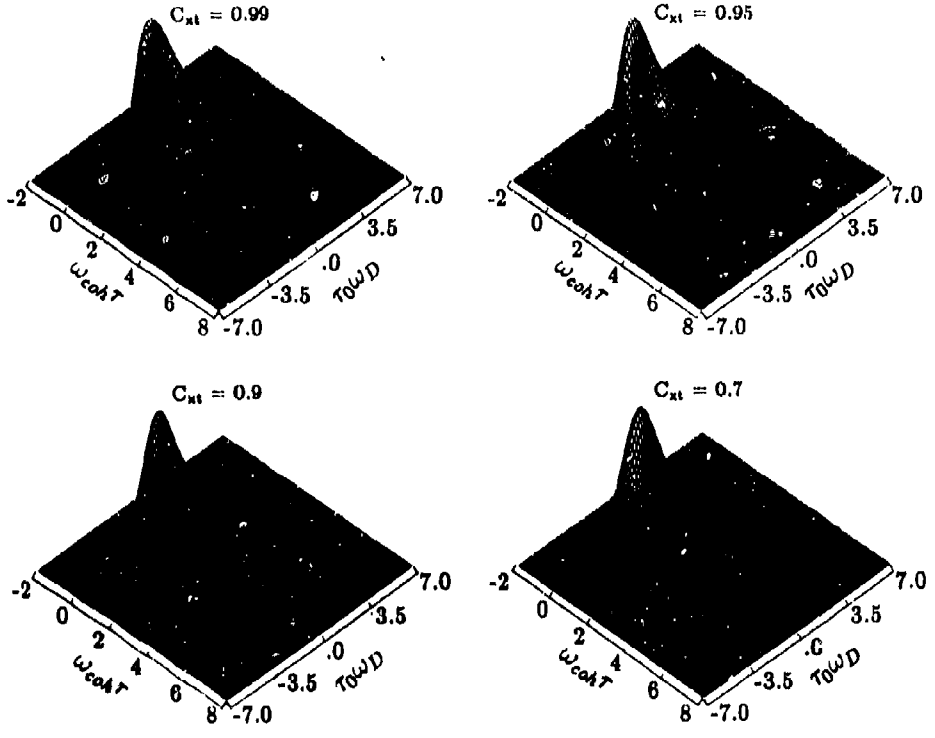

Figure 4. Scattering functions for the general model.

MATCHED FILTER EXAMPLE

Signal scintillation can be either flat fading (nonselective) or frequency selective, depending on the signal bandwidth and the degree ionospheric disturbance. If all frequency components of the received signal vary essentially identically with time, the propagation channel is referred to as nonselective or flat fading. When the scintillations exhibit statistical decorrelation at different frequencies within the signal bandwidth, the channel is referred to as frequency selective. The level of frequency selective scintillation disturbance is measured by the frequency selective bandwidth, f_0. This parameter is defined as

$$f_0 = \frac{1}{2\pi\sigma_\tau} = \frac{\omega_{coh}}{2\pi} \tag{21}$$

where σ_τ is the standard deviation of the time-of-arrival jitter.

Techniques have been developed to generate representative signal structures using statistical channel simulators [Wittwer 1980 and Dana 1986]. The latter reference describes techniques for generating realizations of the channel impulse response function, and describes how these realizations can be used to generate the output of a matched filter. A report is currently in preparation [Dana 1990] that extends these techniques to inlcude the general model.

A comparison of the matched-filter output amplitude generated with the frozen-in, general, and turbulent models is shown in Figure 5 for one level of frequency selective propagation disturbances, characterized by the ratio of the frequency selective bandwidth f_0 to the transmitted chip rate R_c (f_0/R_c = 0.1 for these examples). Each frame provides a three dimensional picture of the matched filter output for a single transmitted pulse as a function of time delay (horizontal scale) and time (scale directed into the figure). The total duration of each of the frames is 10 decorrelation times.

The top frame shows an example generated using the frozen-in model (C_{xt} = 1 and C_{yt} = 0). An effect of the frozen-in model that is evident in the top frame is that the signal arriving at long delays varies more rapidly in time than the signal arriving at shorter delays. The middle frame is a general model realization (C_{xt} = 0.9 and C_{yt} = 0), and the bottom frame is for the turbulent model (C_{xt} = C_{yt} = 0). The difference between the top and bottom frames is that the turbulent model amplitude has the same fading rate at all delays. It can be seen that the general model realization falls somewhere between these two limiting cases.

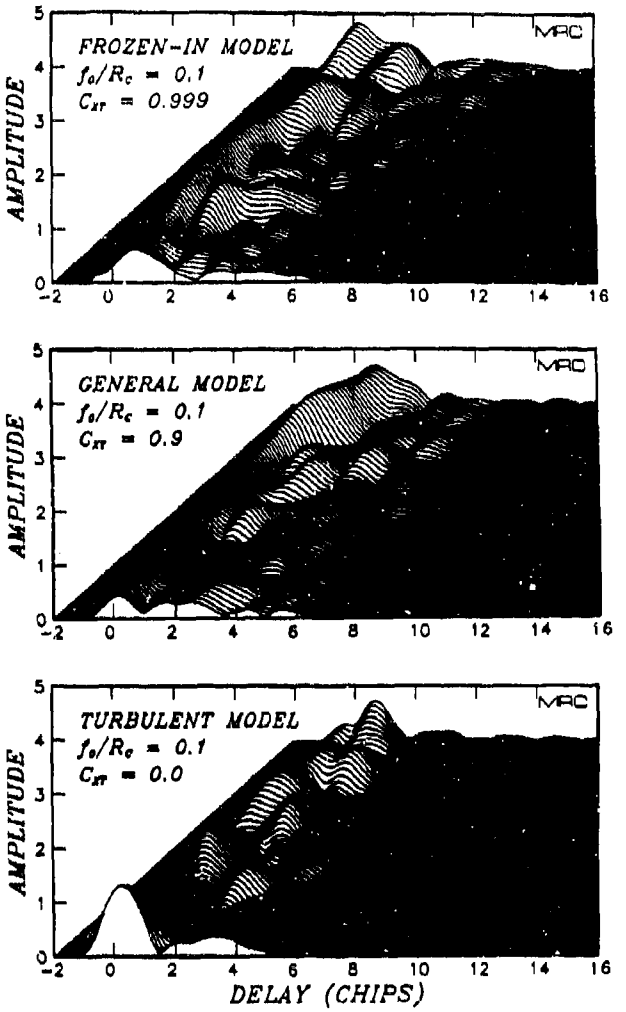

Figure 5. Matched filter output amplitude time histories for frequency selective channels.

ACKNOWLEDGEMENT

This work supported by the Defense Nuclear Agency under contract DNA 001-87-C-0169.

REFERENCES

Dana, R. A., *Propagation of RF Signals Through Structured Ionization. Theory and Antenna Aperture Effect Applications*, DNA-TR-86-158, MRC-R-976, Mission Research Corporation, May 1986.

Dana, R. A., *Propagation of RF Signals Through Structured Ionization. The General Model*, MRC-R-1262, Mission Research Corporation, (in preparation) 1990.

Knepp, D. L., "Analytic Solution for the Two-frequency Mutual Coherence Function for Spherical Wave Propagation," *Radio Science*, Vol. 18, No. 4, pp. 535-549, July 1983.

Sreenivasiah, I., A. Ishimaru, and S. T. Hong, "Two-Frequency Mutual Coherence Function and Pulse Propagation in a Randon Medium: An Analytic Solution to the Plane Wave Case," *Radio Science*, Vol. 11, No. 10, pp. 775-778, October 1976.

Tatarskii, V. I., *The Effects of the Turbulent Atmosphere on Wave Propagation*, translated by Isreal Program for Scientific Translations, National Technical Information Service, U.S. Department of Commerce, 1971.

Wittwer, L. A., *Radio Wave Propagation in Structured Ionization for Satellite Applications*, DNA 5304D, Defense Nuclear Agency, January 1979.

Wittwer, L. A., *A Trans-Ionospheric Signal Specification for Satellite C^3 Applications*, DNA 5662D, Defense Nuclear Agency, December 1980.